A facile precursor route to transition metal molybdates using a polyzwitterionic matrix bearing simultaneously charged moieties and complexing groups†

François Rullens,[a] Nicolas Deligne,[a] André Laschewsky*[bc] and Michel Devillers*[a]

Received 3rd December 2004, Accepted 3rd February 2005
First published as an Advance Article on the web 18th February 2005
DOI: 10.1039/b418233b

An unconventional but easily accessible precursor route involving the thermal treatment of hybrid precursors containing an ampholytic polymer matrix is developed to prepare multimetallic oxides of catalytic interest such as transition metal molybdates. A copolymer of diallyldimethylammonium chloride and a functionalized maleamic acid bearing an amine group suited for cation complexation was designed, synthesized and used as a matrix to stabilize inorganic species generated in solution from $Ni(NO_3)_2{\cdot}6H_2O$, $Co(NO_3)_2{\cdot}6H_2O$ and/or $Mn(NO_3)_2{\cdot}4H_2O$ together with $(NH_4)_6Mo_7O_{24}{\cdot}4H_2O$. UV–vis–NIR as well as ^{13}C-NMR studies suggest that the interactions between the cations and the polymer in solution are mainly electrostatic. Only minor complexation interactions take place under certain conditions. Homogeneous hybrid blends were prepared from these solutions. The presence of a complexing amine group in addition to the charged betaine moieties in the polymer permits stabilization of more than stoichiometric amounts of the metal species in the blends. XRD measurements suggest that the homogeneity in the solid state can be kept up to about 1.5 mol of each metal that is incorporated (anionic as well as cationic) per mol of repeat units of the copolymer. The blends were calcined under air at 600 °C to produce the simple as well as mixed nickel, cobalt and manganese molybdates. Characterization of the final phases by XRD and Raman spectroscopy indicates that the α- as well as the β-molybdate phases can be prepared, and that the mixed structures are solid solutions of the simple $NiMoO_4$, $MnMoO_4$ and $CoMoO_4$. If the precursors engaged are homogeneous, the pH of the precursor solution, the amount of metal that is incorporated in the matrix, and the nature of the polymer matrix seem to exert only a minor influence on the nature of the final phase, which demonstrates the versatility and facile applicability of the method.

1. Introduction

New methods for the preparation of bulk or dispersed mixed oxides exhibiting well-defined characteristics with respect to structure, dispersion of the different components, specific surface area and morphology, are continuously searched for, *e.g.* the production of new efficient catalysts. Among these methods, the precursor routes, based on the decomposition of citrate gels,[1] oxalates,[2] or polyaminocarboxylates like EDTA and its analogs,[3] were successfully used. Alternatively, structurally simple organic polymers such as poly(ethylene glycol),[4] poly(amide) and poly(imide) derivatives,[5] but also more elaborate polymer structures, resulting from the association of monomers bearing carboxylic acid or amine moieties,[6] were occasionally employed to synthesize polymer–metal complexes, which are thermally treated[7] to obtain the inorganic materials. The latter polymers constitute particularly interesting systems for this kind of application because of their tunable properties: solubility in various polar media, number of functional groups of each type, presence of additional substituents able to induce suprastructure or complexation of the cations, *etc*. Up to now, much work has been devoted towards the design of polymers such as poly(betaine)s or poly(ampholyte)s, with the purpose of taking advantage of the presence of electric charges along the chains. These structures make them particularly suited to stabilize and interact with the anions and cations of a soluble inorganic salt by electrostatic[8–11] interactions, to produce homogeneous hybrid materials in the solid state after removal of the solvent. However, the poly(betaine)s designed up to now suffer from a major drawback: the salt-free polymer structures are only obtained *via* multistep reactions, involving tedious purification routes such as the use of ion exchange resins, for example.[12] Next to these considerations, it was not clear whether the presence of additional complexing groups next to the charged moieties of the betaine in a polymer structure could help the stabilization of simple inorganic salts in solution or in the solid state.

Recently, we published first results concerning the development of a new synthetic pathway to multimetallic oxides, based on the use of hybrid inorganic–organic mixtures made from simple inorganic salts and an ordered and regular

† Electronic supplementary information (ESI) available: Electronic spectra and UV–vis–NIR absorbance maxima for Ni^{++} solutions. See http://www.rsc.org/suppdata/jm/b4/b418233b/

*andre.laschewsky@iap.fhg.de (André Laschewsky)
devillers@chim.ucl.ac.be (Michel Devillers)

poly(ampholyte) matrix.[13] The polymer used in that previous work, namely poly(*N*,*N*-diallyl-*N*-hexylamine-*alt*-maleic acid), was prepared by multistep synthesis and a complex purification procedure to avoid the presence of residual inorganic salts in the structure.[14] We describe in this paper further investigations carried out in order to optimize this approach, and make it easier to implement in the context of catalysts design and preparation. Because the organic polymer used serves as a sacrificial matrix to prepare oxides, the purpose is to develop a very facile synthetic route to an appropriate organic polymer matrix, which is able to stabilize efficiently cationic as well as anionic metal species. This was achieved by choosing a commercial cationic monomer together with a functional, most easily accessible maleamic acid. Different from our first approach,[14] the polymer is made now from a hydrolytically stable quaternized, *i.e.* permanently cationic, ammonium monomer which enables strong electrostatic interactions with anions at any pH value. Also, the polymer behaves as a polyzwitterion in a large pH window. Additionally to the betaine groups, the new polymer prepared exhibits a piperazine moiety in its repeat unit, which is known to be efficient for cation complexation, either if present in the side group or in the main chain of a macromolecule.[15–17] Because the influence of an additional complexing group on the stabilization of inorganic species in the polymer–salt blends was not clear from the literature, this point was elucidated. A detailed description of the interactions between the organic matrix and the inorganic species in solution as well as in the solid state is given, in order to propose a realistic model for the incorporation of cationic as well as anionic metal species in the polymer blend. Our strategy is broadened to the preparation of various transition metal molybdates (Mn, Ni, Co) that can be used as catalysts in selective oxidations.[18,19] Finally, we were interested in checking the influence of different experimental parameters on the nature of the final phase that is obtained, as the nature of the polymer matrix, the relative amount of metal and polymer and the pH of the precursor solutions.

2. Experimental

2.1. Materials

Solvents used, namely *n*-pentane (Fischer Scientific) and methanol (Fischer Chemicals), were analytical reagent grade. Concentrated hydrochloric acid (37 wt.% in water) was supplied from Fisher Scientific. Diallyldimethylammonium chloride (DADMAC, 65 wt.% in water) was purchased from Aldrich. Maleic anhydride was supplied from Fluka Chemika. 1-Methylpiperazine, succinic acid, cobalt(II) nitrate hexahydrate and ammonium heptamolybdate(VI) tetrahydrate were purchased from Acros Organics and used without further purification. Nickel(II) nitrate hexahydrate was supplied from Janssen Chimica. Manganese(II) nitrate tetrahydrate was purchased from Alfa Aesar. 2,2′-Azobis[2-methyl-*N*-(2-hydroxyethyl)propionamide] (VA086) was supplied from Wako. Water used during synthesis and purification steps was first purified using an Elgastat Maxima system (resistance: 18.2 MΩ). Spectra/Por dialysis membranes (nominal cut-off: 2000 Da) were employed for polymer purification.

2.2. Methods

Standard ^{1}H- and ^{13}C-NMR spectra were taken on a Varian Gemini 200 MHz spectrometer. ^{13}C experiments (APT, (semi)quantitative spectra) were performed on a 500 MHz spectrometer (Bruker, Avance 500). ^{1}H chemical shifts were calibrated to the residual signals of the solvents for D_2O (4.63 ppm) and CD_3OD (3.3 ppm). For ^{13}C-NMR spectra, sodium 2,2-dimethyl-2-silapentane-5-sulfonate (DSS) was employed as external reference for chemical shifts in D_2O, and residual proton signal from CD_3OD (49.1 ppm) was used as internal standard. FTIR spectra of the products in KBr pellets (1 wt.%) were recorded on a Biorad FTS135 spectrometer. Elemental analysis was carried out at University College, London, UK. ICP analysis was performed at the analytical laboratory of the Fraunhofer-Institute for Applied Polymer Research. The TGA curves were recorded under air atmosphere on a Mettler-Toledo 851e thermogravimetric analyser, applying a heating rate of 10 °C min^{-1}. Solution UV–vis–NIR measurements were performed on a Varian Cary 5E. Powder X-ray diffractograms (XRD) were taken with a Siemens D5000 diffractometer, using the Cu Kα line (λ = 0.1541 nm). Raman spectra were taken on a Bruker RFS100/S spectrometer, at a wavelength of 1064 nm. Scanning electron microscopy (SEM) was performed with a Gemini DSM 982 digital scanning microscope. The hybrid materials were successfully analyzed by deposition of Cr at the surface of the samples using a plasma, in order to increase their conductivity.

2.3. Synthesis of comonomer and polymerization

(4′-Methyl-piperazinyl)-4-oxo-2-butenoic acid. 20.03 g (200.0 mmol) of *N*-methyl piperazine were added dropwise to a solution of 19.62 g (200.1 mmol) of maleic anhydride in 20 ml of acetone at 0 °C. A precipitate formed rapidly. The solvent was evaporated, the residue was dissolved in 100 ml of a mixture of ethanol–water [70 : 30 (v : v)]. After several precipitations into pentane, the precipitate was isolated by filtration, and dried overnight *in vacuo* at 50 °C, to give 34.9 g (yield: 88%) of white powder. ^{1}H-NMR (200 MHz, CD_3OD): δ (ppm): 6.20 (d; 1H, =CH–COOH); 6.05 (d; 1H, –N–C(=O)–CH=); 3.85–3.60 (m; 4H, –C(=O)–N–CH_2–); 3.26–3.06 (m; 4H, –C(=O)–N–C–CH_2–N); 2.77 (s; 3H, –CH_3). ^{13}C-NMR (50 MHz, CD_3OD): δ (ppm): 171.8 (–*C*OOH); 170.6 (–N–*C*(=O)–); 132.8 (=*C*H–COOH); 131.6 (–N–C(=O)–*C*H=); 53.6 (–*C*H_2–N–CH_3); 44.9 (–C(=O)–N–*C*H_2–, *cis*-position of the amide); 43.7 (N–*C*H_3); 39.8 (–C(=O)–N–*C*H_2–, *trans*-position of the amide). MS (APCI): 199.2 $[M+1]^+$.

Poly[*N*,*N*-dimethyl-*N*,*N*-diallylammmonium chloride-*alt*-(4′-methyl-piperazinyl)-4-oxo-2-butenoic acid] (inner salt). 105.8 g of (4′-methyl-piperazinyl)-4-oxo-2-butenoic acid (533.7 mol) were dissolved in 132.8 g of a 65 wt.% aqueous solution of DADMAC (533.9 mol), by adding 50 g of water and adjusting the pH value to 8 with 0.5 M aqueous NaOH. After the adding of the initiator (VA086, 10 mol.% to monomers), the homogeneous solution was degassed by six freeze-and-thaw cycles, and reacted at 75 °C during 48 h. After cooling, the crude solution was dialyzed, first in aqueous HCl (pH = 2) for 7 days, and subsequently in pure water for 5 days,

changing the solvent every day. The solution was lyophilized to yield 31 g (18%) of a yellowish solid. ^{1}H-NMR (300 MHz, D_2O): δ (ppm): 4.20–3.41 (4H; –N^+–CH_2–); 3.41–2.86 (10H, N^+–CH_3 and C(=O)N–CH_2); 2.86–0.80 (15 H; backbone, H_3C–N–CH_2–). ^{13}C-NMR, APT sequence (125MHz, D_2O): δ (ppm): 183.2 (*C*(=O)OH); 176.8 (–*C*(=O)N–); 75.4, 73.8 (N^+–*C*H_2); 57.5, 55.3, 53.9 (N^+–*C*H_3); 47.5, 44.5, 43.6 (C(=O)N–*C*H_2–*C*H_2–); 46.7, 46.1, 45.0, 41.4, 41.0 (–*C*H– backbone, –*C*H–C(=O), >N–*C*H_3); 32.9, 29.2 (–*C*H_2– backbone). FTIR (KBr) selected bands (cm^{-1}): 3025, 2940, 2862, 2809 ($\nu_{sym+asym}$ CH_3, CH_2, CH); 1630 (ν C=O in C(=O)NR_2), 1577 (ν_{asym} C=O in COO^-), 1470 (δ_{sym} CH_2 and δ_{asym} CH_3), 1394 (δ_{sym} CH_3 and ν_{sym} C=O in COO^-). Elem. Anal. Calcd. for $C_{17}H_{29}N_3O_3$ (M = 324.20) C 63.11 H N 12.99 Cl 0 C/N ratio 4.853; Found C 54.70 H 8.51 N 11.27 Cl 0.01 C/N ratio 4.854. Na content (ICP): below 0.01%.

2.4. Preparation of the hybrid materials

In a typical experiment, 100 mg of polymer were dissolved in 25 ml of water by stirring at room temperature. The appropriate amounts of 0.1 M aqueous solutions (pH = 10) of the inorganic species ($Ni(NO_3)_2{\cdot}6H_2O$, $Mn(NO_3)_2{\cdot}4H_2O$, $Co(NO_3)_2{\cdot}6H_2O$ and $(NH_4)_6Mo_7O_{24}{\cdot}4H_2O$) were added in order to reach the desired molar ratio of metal ion(s) per repeat unit of copolymer. The pH value was adjusted by adding an appropriate amount of 0.1 M aqueous NH_3 or HNO_3. The solution was stirred for 30 min, and finally lyophilized to produce coloured, finely divided powders.

3. Results and discussion

3.1. Synthesis of polymer matrix

The polymer was prepared in analogy to a literature procedure,[20] by copolymerizing the commercially available diallyldimethylammonium chloride with an unsaturated amino acid, namely the maleamic acid that is prepared by ring-opening addition of *N*-methyl piperazine onto maleic anhydride (Fig. 1). Copolymer yields are typically in the range of 15–20%, but as far as the monomers are really easily accessible, this point does not constitute a major drawback in this context. Whereas ^{1}H-NMR spectra are complex due to the superposition of broad signals, ^{13}C-NMR spectra of the copolymer are more instructive, and show the signals of COO^-, amide and ammonium moieties in the structure. The presence of the functional COO^- and amide moieties is corroborated by characteristic signals in the FTIR spectra. Elemental analysis indicates that the copolymer contains equimolar amounts of

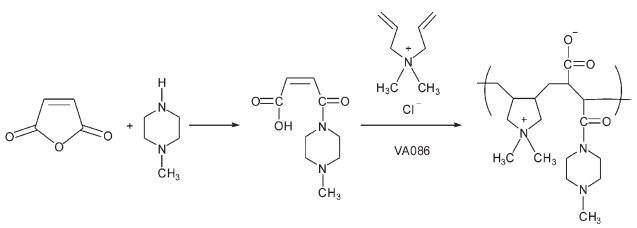

Fig. 1 Facile synthetic route to the precursor monomer and copolymer matrix.

both monomers even at low conversions, as indicative for a strictly alternating copolymerization. This is in agreement with the scarce reports on the copolymerization of diallyldimethylammonium chloride with maleamic acids,[20] and matches well with the alternating copolymerization found for diallylammonium salts or diallylamine derivatives and maleic acid.[14,21,22] The extensive dialysis of the copolymers at neutral pH produces copolymers that are free of inorganic ions, namely of sodium and chloride, as carefully checked by elemental analysis and ICP. This purification produced therefore a salt-free zwitterionic copolymer of the carboxybetaine type, as was considered important in order to avoid contamination of the mixed organic and inorganic hybrid materials prepared from this copolymer by incorporation of selected inorganic species. Finally, the structure of the copolymer makes it well-suited for interacting with inorganic compounds *via* electrostatic (due to the presence of carboxylate and ammonium moieties), but also *via* complexation interactions (due to the presence of the *N*-methyl piperazine group).

3.2. Solution studies of precursors

Preliminary miscibility tests in solution of the organic matrix with the inorganic salts were carried out first. $Ni(NO_3)_2{\cdot}6H_2O$, $Mn(NO_3)_2{\cdot}4H_2O$ and $Co(NO_3)_2{\cdot}6H_2O$ were incorporated alone or together with $(NH_4)_6Mo_7O_{24}{\cdot}4H_2O$ under determined pH conditions, in presence of the polymer. The homogeneity of the solutions was checked by a qualitative appreciation of the transparency of the solution. The general trend indicates that homogeneous solutions can be produced throughout the whole pH range. To determine which kind of interactions stabilize the organic polymer, bearing simultaneously charged moieties and complexing groups, and the cationic inorganic species in solution, UV–vis–NIR studies were undertaken, using different kinds of hypothetical ligands for the Ni(II) and Co(II) ions. Next to the polymer, the precursor monomer, *N*-methyl piperazine and succinic acid were tested. For a given pH value of about 10.4, a slight shift of the absorption bands between a reference spectrum of Ni^{++} in presence of ammonia on the one hand, and the spectra of Ni^{++} together with *N*-methyl piperazine or (4′-methylpiperazinyl)-4-oxo-2-butenoic acid on the other hand, is observed (*cf.* Fig. S1 in the electronic supplementary information (ESI)†). This suggests the existence of complexation interactions between the cation and the amine moieties of the ligands. On the other hand, no shift was found in the presence of succinic acid or the polymer employed as hypothetical ligands, but this finding does not indicate that no complexation occurs. In order to evidence a possible influence of pH on the interactions between the matrix and Ni^{++} in solution, spectra of the two species at different pH values were recorded (*cf.* Table S1 in the ESI†). The maxima of absorbance from the spectra of Ni^{++} in presence of polymer, for different basic pH values in order to ensure sufficient deprotonation of the amine group, were collected and compared with the corresponding data from the reference spectra. Slight shifts between reference and polymer solutions spectra are observed at pH values of 9.2 and 9.8, suggesting the occurrence of complexation interactions. On the other hand, no complexation can be evidenced when the pH value is raised

or reduced (namely pH = 8.4, 10.4 or 11.6). The same experiments were carried out using Co^{++}, but the spectra did not prove the existence of complexation in solution between the polymer and the cation, at least at pH values from 2 to 9.2. Precipitation of the chelate occurred if the pH was subsequently increased, which limited the obtained information. Similar studies could not be carried out with the Mn^{++} solutions, because of the absence of any spin-allowed d–d transition in high-spin octahedral d^5 complexes.

In addition, solution ^{13}C-NMR has been implemented in the case of the Ni^{++} ion, in order to get complementary information which can not be obtained from UV–vis spectroscopy, namely about the nature of the interactions between the carboxylate moiety and the cation. Fig. 2 compares the ^{13}C-NMR spectra of the prepared monomer and copolymer with the spectra of the same species in the presence of $Ni(NO_3)_2{\cdot}6H_2O$, at a fixed pH value of 10. Spectra of the monomer together with Ni^{++} exhibit a shift downfield of all peaks in the spectrum, compared with the spectrum of the salt-free monomer, combined with a broadening of the signals at 178 ppm and 141 ppm, attributed to amide and carboxylate and the double bond. This means that the paramagnetic Ni^{++} species preferably interacts in aqueous solution with these groups, *via* complexation interactions in the case of COO^-. In the same way, the peak at 183 ppm, attributed to the carboxylate moiety in the copolymer, broadens when 0.5 mol of metal per mol of repeat units of the polymer is added, compared with the spectrum of the salt-free copolymer. Here, no significant shift of the other peaks in the spectrum can be evidenced, which suggests that the major interactions between Ni^{++} and the matrix are probably mainly electrostatic. If the amount of salt is increased up to equimolar quantities of metal cation and repeat units of the polymer, broadening of all the signals appears, due to the presence of a paramagnetic species which dramatically diminishes the relaxation times of all nuclei. As a consequence, the general trend from these UV–vis–NIR and NMR studies suggests that the interactions between the cations and the polymer in a basic solution are essentially of electrostatic nature, even if additional complexation involving the piperazine group is thought to take place under some conditions.

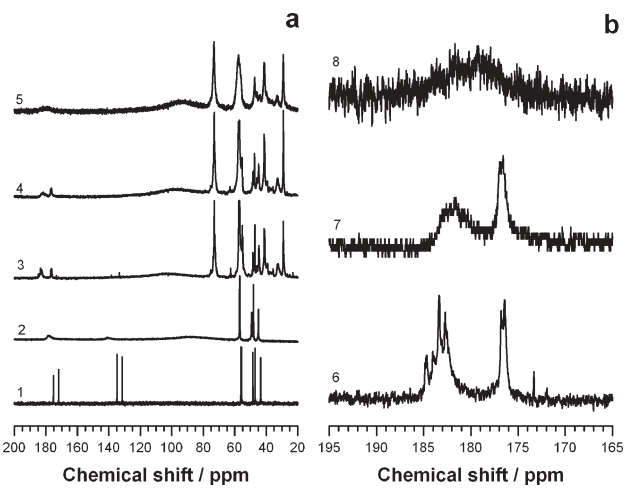

Fig. 2 (a) Semi-quantitative ^{13}C NMR spectra in D_2O (pH = 10) of (4′-methyl-piperazinyl)-4-oxo-2-butenoic acid (1), (4′-methyl-piperazinyl)-4-oxo-2-butenoic acid in the presence of $Ni(NO_3)_2{\cdot}6H_2O$ (molar ratio: 1 mol of ligand for 0.5 mol of metal cation) (2), the salt-free copolymer (3), and the copolymer in presence of $Ni(NO_3)_2{\cdot}6H_2O$ (molar ratios: 0.5 mol (4) and 1 mol (5) of metal cation per mol of repeat units of the copolymer); (b) magnified parts (spectra 6, 7 and 8) of spectra 3, 4 and 5, respectively, illustrating the carbonyl signals from amide and carboxylic moieties.

3.3. Solid state studies of precursors

In order to prepare homogeneous hybrid mixtures made from the synthetic polymer and the selected inorganic salts, a systematic screening of the homogeneity of the materials in the solid state was carried out using powder XRD. Test samples were at first prepared by mixing and grinding in the solid state the polymer with each of the inorganic salts, in a molar ratio of repeat units of polymer relatively to the inorganic metals of 1 to 0.1, to get powders. Sharp lines which indicate the presence of phase-separated inorganic salts were observed in the diffractograms of these powders, *i.e.* the mixtures were not homogeneous. This finding demonstrates also that XRD measurements are appropriate to check the eventual inhomogeneity of the samples, even if only a small amount of inorganic species does not sufficiently interact with the polymer matrix. In order to obtain homogeneous mixtures, hybrid materials were prepared in solution, lyophilized and analyzed by XRD. Fig. 3 compares the XRD pattern of the polymer with the diffractograms of hybrid materials made from the polymer and $Co(NO_3)_2{\cdot}6H_2O$ together with $(NH_4)_6Mo_7O_{24}{\cdot}4H_2O$, obtained from solutions prepared at different pH values, and for different amounts of salts incorporated. The results indicate that the materials prepared from aqueous solutions at a pH value of 10 are homogeneous when the total molar amount of inorganic salts introduced

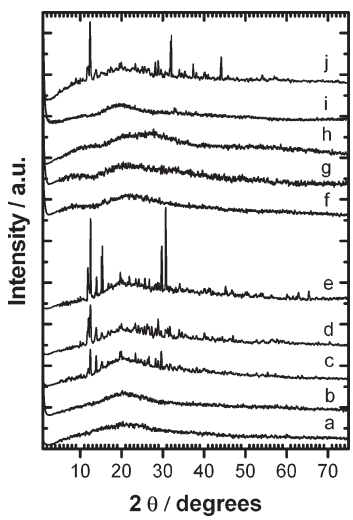

Fig. 3 XRD patterns of the polymer (a) and hybrid blends made from the polymer and different amounts of $Co(NO_3)_2{\cdot}6H_2O$ and $(NH_4)_6Mo_7O_{24}{\cdot}4H_2O$ and prepared at different pH values: from (b) to (e): pH = 2; 0.25, 0.5, 1 and 2 mol of each metal ion per mol of repeat units of the copolymer; from (f) to (j): pH = 10; 0.25, 0.5, 1, 1.5 and 2 mol of each metal ion per mol of repeat units of polymer.

is up to 1.5 mol of each metal per mol of repeat units of polymer. A pH value of 2 is not suitable for obtaining homogeneous materials, unless only 0.25 mol of each metal is incorporated. This is most probably due to the high degree of protonation of the carboxylate moiety under these conditions, but also to the presence of bulky Mo(VI) species such as $[Mo_7O_{24}]^{6-}$ or $[Mo_8O_{26}]^{4-}$ under these acidic conditions.[23] The difficulty of these bulky species to interact with the matrix probably contributes to the loss of homogeneity. Attempts have been made to identify the phase containing the residual inorganic salt which did not interact with the polymer, by comparison of the XRD patterns with JCPDS files of the precursor inorganic materials, and by using Raman spectroscopy, but without any success. Globally, the general trend demonstrates that 1 mol of cationic as well as anionic metal species per mol of repeat units of polymer can be easily blended under basic conditions. This is due to the presence of the carboxylate and ammonium moieties in the matrix structure, and is in agreement with previous observations on similar systems.[13,24] However, 0.5 additional mol of metal species per mol of repeat units of the polymer can be blended in the matrix to produce homogeneous materials. This result indicates that, in addition to the carboxylate group, another moiety takes part in the subsequent stabilization of Co(II) in the solid state. Next to the carboxylates, the amido or more probably amino groups from the piperazine moieties probably interact with the cationic inorganic species. This is in line with a similar observation in the literature[25] concerning the auxiliary stabilization in the solid state of low molar mass salts in conventional poly(betaine) systems whose structure exhibits atoms bearing lone electron pairs. For example, it has been shown that poly(sulfobetaine)s based on poly(acrylamide) allow higher salt contents than the analogous poly(methacrylate). In this case, the excess of anionic molybdates are assumed to rearrange themselves around positively charged entities in the system, which produces a homogeneous blend. As expected, the structure of the polymer has indeed a major effect on the mixing behaviour with inorganic salts. Globally, however, when 1 mol of each metal is incorporated in the matrix under basic conditions, a simple model based on electrostatic interactions between the inorganic species (anionic as well as cationic) and the charged moieties of the polymer permits the explanation of the formation of homogeneous materials in the solid state (Fig. 4). Additionally, SEM was implemented to look for eventual correlations between the (in)homogeneity of the materials and the morphology of the particles. Fig. 5 illustrates typical micrographs of (in)homogeneous materials. Spherical particles and aggregates of sphere-like particles are mainly detected on the micrographs of the materials prepared

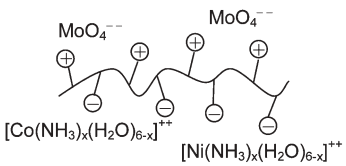

Fig. 4 Schematic representation of the incorporation of anionic as well as cationic metal species in a zwitterionic polymer, leading to the formation of a homogeneous hybrid material.

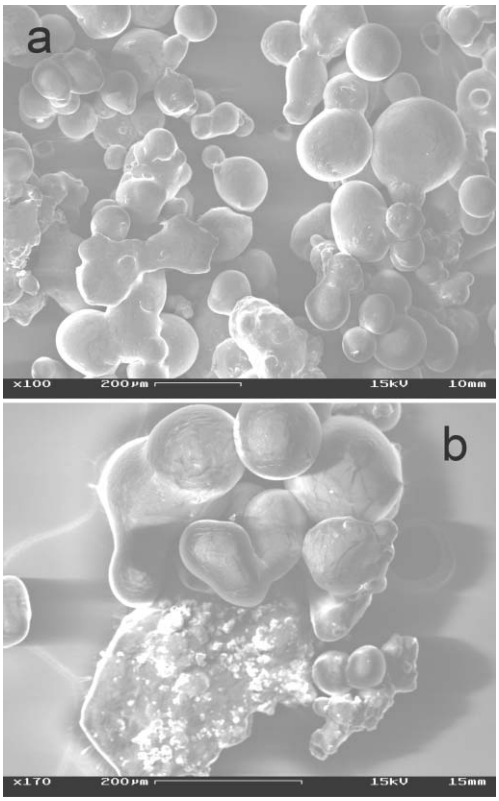

Fig. 5 Typical SEM micrographs (magnification: 100×) of homogeneous (a) and inhomogeneous (b) materials made from the polymer and $Ni(NO_3)_2{\cdot}6H_2O$ incorporated jointly with $(NH_4)_6Mo_7O_{24}{\cdot}4H_2O$; pH of the precursor solution: 10 (a) and 4 (b).

under basic pH conditions. However, the morphology of the particles is quite different in the case of materials prepared under acidic conditions: next to the same sphere-like particles isolated for the materials prepared under basic conditions, particles exhibiting various shapes are also typically present in the micrographs. This is a further piece of evidence of the formation of a separate phase under acidic conditions, leading to an inhomogeneous material.

3.4. Thermal behaviour of the precursors

Thermal decomposition of the organic matrix and formation of the oxide phases were followed by thermogravimetric analysis (TGA). Fig. 6 displays the TGA curves of hybrid materials made from $Ni(NO_3)_2{\cdot}6H_2O$, $Co(NO_3)_2{\cdot}6H_2O$ and $(NH_4)_6Mo_7O_{24}{\cdot}4H_2O$. All curves exhibit a first weight loss between 50 °C and 100 °C, which is attributed to dehydration of the material. This is followed by different steps corresponding to the pyrolysis of the matrix above 200 °C, which is combined with the degradation of the nitrate counter-ions and the formation of the expected oxide phase. The weight becomes stable from ~570 °C, and up to 850 °C. The pyrolysis of the matrix is nearly complete, as the residual weights match well with the values calculated on the basis of the formation of the corresponding molybdates, which indicates, as expected, that the main degradation products consist of the pure simple or mixed Ni and/or Co molybdates which are free of contaminants. The residual C, H and N contents in the final

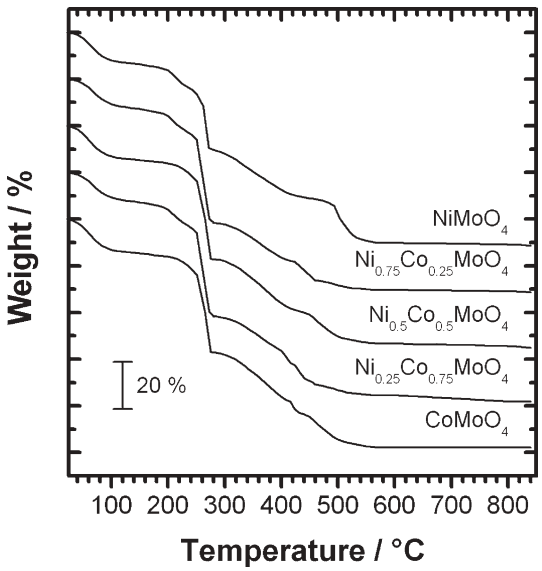

Fig. 6 TGA curves under air of different hybrid materials containing $Ni(NO_3)_2{\cdot}6H_2O$ and $(NH_4)_6Mo_7O_{24}{\cdot}4H_2O$ (0.5 mol of metal ions per mol of repeat units of the polymer), whose degradation products correspond to the simple or mixed Ni and/or Co molybdates.

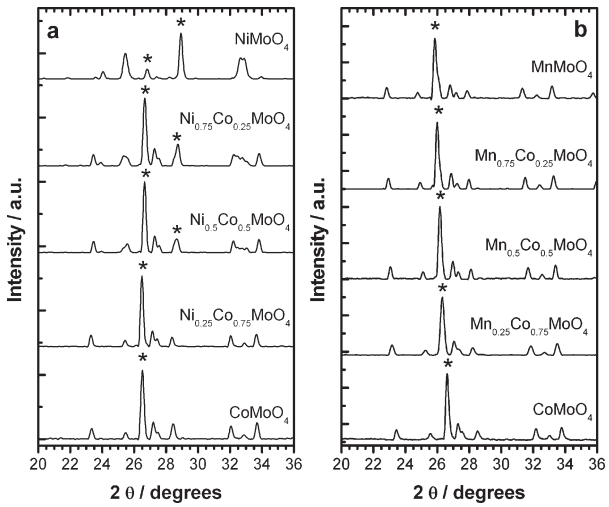

Fig. 7 Typical X-ray diffractograms of the simple and mixed Ni and/or Co molybdates (a) and Mn and/or Co molybdates (b). The star denotes the position of the (220) reflection, corresponding to α- and/or β-phase.

products were checked by elemental analysis (Table 1). The C content is typically below 0.5%, which demonstrates that the method is efficient to produce inorganic materials really free of organic contaminants.

3.5. Preparation and characterization of the final molybdate phases

According to the thermal behaviour of the hybrid precursors, inorganic materials were prepared upon calcination of the precursors under an air flow of 1 L min^{-1} at 600 °C, namely about 30 °C higher than the final decomposition temperature of the hybrid blends determined by TGA, in order to ensure the complete pyrolysis of the organic matrix and favour the formation of the crystalline phases.

3.5.1. Simple and mixed nickel and cobalt molybdates. Different sets of simple and mixed nickel and cobalt molybdates with the general formula $Ni_{1-x}Co_xMoO_4$, where x = 0, 0.25, 0.5, 0.75, (0.9) and 1, were prepared according to the developed method. Systematic preparations were performed in order to check the influence of the pH of the precursor solution and the amount of inorganic salt introduced under defined pH conditions on the nature of the formed oxide phase. Fig. 7a illustrates the XRD patterns of a series of final oxide materials, obtained from precursor solutions prepared at a pH value of 7, and whose composition corresponds to 0.5 mol of metals per mol of repeat units of copolymer. The nature of the molybdate phase (α-, β- or mixture) was determined as described previously,[26–31] by the position of specific XRD lines in the range 20–36°, referring to the corresponding JCPDS files (α-$NiMoO_4$: file 33-0948, β-$NiMoO_4$: file 45-0142, β-$CoMoO_4$: file 21-0868). The evolution of the diffractograms as a function of the relative amount of Ni^{++} and Co^{++} for the different series of nickel and cobalt molybdates is quite similar. Fig. 8a displays the evolution of the corresponding interreticular spacings calculated from the positions of the (220) reflections as a function of the Ni and Co composition in $Ni_{1-x}Co_xMoO_4$. A mixture of the α-phase (mainly) and the β-phase of $NiMoO_4$ on the one hand, and the pure β-$CoMoO_4$ on the other, are obtained in the case of the two simple oxides, whatever the pH studied and the amount of salt introduced. The mixed nickel and cobalt molybdates are identified as mixtures of the α- and β-phases (x = 0.25 and 0.5 for pH values of 7 and 10; x = 0.25, 0.5 and 0.75 for a pH value of 12) or as the pure β-phase (x = 0.75 at a pH value of 7; x = 0.75 and 0.90 for a pH value of 10), whatever the amount of inorganic species introduced in the precursor. Vegard's law appears to be respected in two different composition domains. Subsequently, shifts in the d(220) values calculated from the peaks' positions in the diffractograms are observed going from α-$NiMoO_4$ to α-$Ni_{0.5}Co_{0.5}MoO_4$ (pH = 7, 10) or from α-$NiMoO_4$ to α-$Ni_{0.25}Co_{0.75}MoO_4$ (pH = 12), and from β-$NiMoO_4$ to β-$CoMoO_4$. This behaviour is consistent with a lattice expansion of the molybdate network with increasing Co content, reflected by the linear increase of the d(220) spacing with the Co–Ni ratio across each region, and is in agreement with the increase of the ionic radius of the six-fold coordinated ions, going from Ni^{++} to Co^{++}. Since both the cell dimensions and the relative intensities vary linearly with the Ni–Co atomic ratio, application of Vegard's law led to the conclusion that the structures of the mixed nickel–cobalt molybdates in each domain are solid solutions of α-$NiMoO_4$ and α-$CoMoO_4$ on

Table 1 Residual C, H and N contents for some prepared simple and mixed Ni and/or Co molybdates.

Sample	% C	% H	% N
$NiMoO_4$	0.23	0	0
$Ni_{0.75}Co_{0.25}MoO_4$	0.22	0.03	0
$Ni_{0.5}Co_{0.5}MoO_4$	0.34	0.05	0
$Ni_{0.25}Co_{0.75}MoO_4$	0.21	0.03	0
$CoMoO_4$	0.35	0.06	0

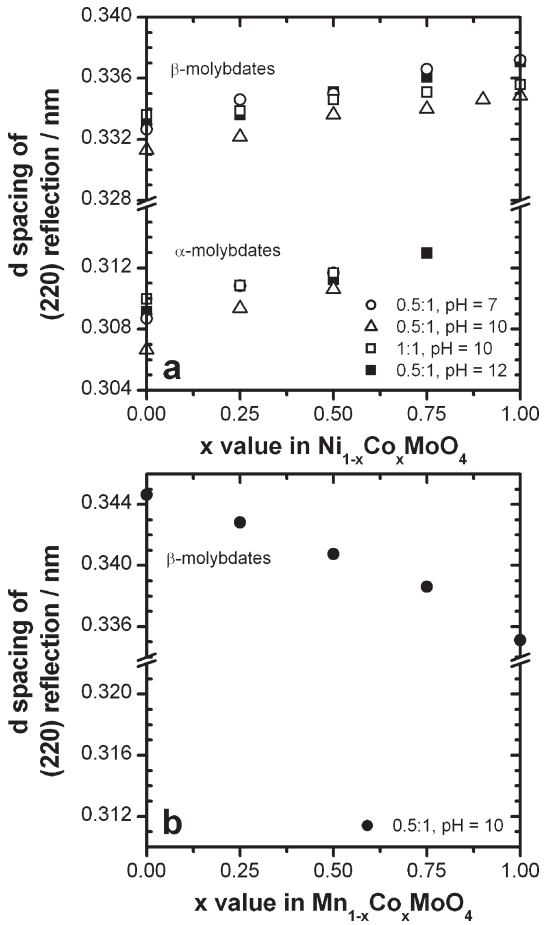

Fig. 8 Verification of Vegard's law on the basis of the interreticular distances corresponding to (220) reflections for different sets of simple and mixed molybdates, as a function of the experimental conditions: (a) $Ni_{1-x}Co_xMoO_4$ phases prepared at different pH values of the precursor solution (pH = 7, 10 and 12) and from precursors containing different amounts of metal ions (0.5 and 1 mol of metal ions per mol of repeat units of the copolymer); (b) $Mn_{1-x}Co_xMoO_4$ phases prepared at a pH value of the precursor solution of 10 and from precursors containing 0.5 mol of metal ions per mol of repeat units of the copolymer.

the one hand, and β-$NiMoO_4$ and β-$CoMoO_4$ on the other, in a common molybdate lattice. In addition to the XRD measurements, the materials were investigated by Raman spectroscopy, in order to confirm the nature of the phases. The Raman spectra of the materials prepared at a pH value of 10 and from precursors containing 0.5 mol of metals per mol of repeat units of polymer are given at Fig. 9a. These data were analyzed with the help of literature data.[32–35] $NiMoO_4$ is identified by the presence of lines at 961 cm^{-1}, 713 cm^{-1} and 705 cm^{-1} on the spectra, corresponding to the so-called α′-phase, which is a distorted form of α-$NiMoO_4$, obtained due to the grinding of the sample. Spectra of the mixed molybdates also exhibit intense lines at around 700 cm^{-1}, which are normally typical of the α-phase. In the same way, the absence of this band in the spectrum of $CoMoO_4$ suggests that the β-phase is produced. Finally, the two neighbour lines at about 940 cm^{-1} resulting in a poorly-resolved broad band, reveal the occurrence of the β-phase. As a whole, these results

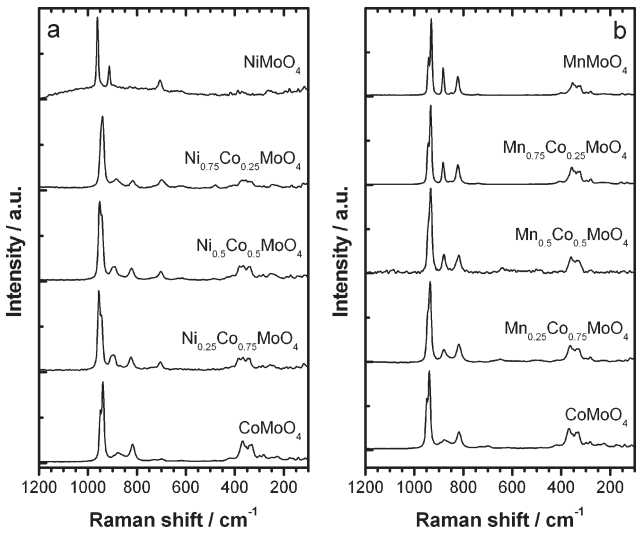

Fig. 9 Typical Raman spectra of the simple and mixed Ni and/or Co molybdates (a) and Mn and/or Co molybdates (b).

are in perfect accordance with those obtained by XRD measurements. In conclusion, the pH of the precursor solution and the amount of metal introduced under defined pH conditions have, under the chosen preparation conditions, little influence on the nature of the generated phase of the molybdates.

3.5.2. Simple and mixed manganese and cobalt molybdates. The same procedure was applied to the preparation of simple and mixed manganese and cobalt molybdates, corresponding to the formulation $Mn_{1-x}Co_xMoO_4$, where x = 0, 0.25, 0.5, 0.75 and 1. The materials were obtained from precursor solutions prepared at a pH value of 10, and of relative composition of 0.5 mol of metals per mol of repeat units of copolymer. The X-ray diffractograms (Fig. 7b) demonstrate that the simple $CoMoO_4$ and the mixed Mn and Co molybdates are obtained in the form of their β-phase. The structure of the simple $MnMoO_4$ was identified in the same way in agreement with the JCPDS data (file 82-2166),[35] to be the α-$MnMoO_4$, which is in fact isomorphous to β-$NiMoO_4$ and β-$CoMoO_4$.[27] Fig. 8b displays the evolution of the interreticular spacing d(220) as a function of the composition of $Mn_{1-x}Co_xMoO_4$. Vegard's law is respected through the whole composition range. Subsequently, shifts in the d(220) values are observed going from α-$MnMoO_4$ to β-$CoMoO_4$. In this case, the behaviour is consistent with a lattice contraction of the molybdate network with increasing Co content, reflected by the linear decrease of the d(220) spacing with increasing Co–Mn ratio, and is in agreement with the decrease of the six-fold coordinated ionic radii from Mn^{++} to Co^{++}. Since both the cell dimensions and the relative intensities vary linearly with the Mn–Co atomic ratio, application of Vegard's law led in this case to the conclusion that the structures of the mixed manganese–cobalt molybdates are solid solutions of α-$MnMoO_4$ and β-$CoMoO_4$ in a common molybdate lattice.[36] Again, Raman spectroscopy confirmed the nature of the phases. Spectra of the materials are given at Fig. 9b. The spectrum of the pure α-$MnMoO_4$ exhibits well-defined lines at

942 cm^{-1}, 931 cm^{-1}, 882 cm^{-1}, 822 cm^{-1}, 354 cm^{-1}, 323 cm^{-1} and 281 cm^{-1}, which is in perfect agreement with the literature data.[37] Spectra of the mixed Mn and Co molybdates show typical lines in the range 936 cm^{-1}–932 cm^{-1} (two neighbouring lines resulting in a broad band with poor resolution), 882 cm^{-1}–878 cm^{-1}, 823 cm^{-1}–817 cm^{-1}, 364 cm^{-1}–358 cm^{-1}, 333 cm^{-1}–326 cm^{-1} and 291 cm^{-1}–278 cm^{-1}.

4. Conclusions

An unconventional synthetic approach, based on the use of hybrid precursors made from inorganic salts and a water-soluble organic polymer, was applied to the preparation of simple and mixed transition metal molybdates. Because the polymer serves as sacrificial matrix, a facile synthetic route to an appropriate polymer was developed. Hybrid precursor blends were prepared from aqueous solutions, the polymer stabilizing the inorganic species generated in solution by the incorporation of $Ni(NO_3)_2{\cdot}6H_2O$, $Mn(NO_3)_2{\cdot}4H_2O$, $Co(NO_3)_2{\cdot}6H_2O$ and $(NH_4)_6Mo_7O_{24}{\cdot}4H_2O$ under the appropriate conditions. The interactions in solution between the polymer matrix and the inorganic species (anionic as well as cationic) are mainly of an electrostatic nature, even if complexation can be evidenced under some determined conditions. Solid homogeneous organic–inorganic hybrid blends can be prepared from these solutions, incorporating up to 1.5 mol of each metal (anionic as well as cationic species) per mol of repeat unit of the copolymer. This finding clearly demonstrates the advantage of using a copolymer bearing an additional complexing group as organic matrix, compared to previously used standard poly(betaine) systems. Subsequent calcination of the homogeneous mixtures under air produces the corresponding simple and mixed nickel, cobalt and/or manganese molybdates, in the form of their α- and/or β-phases. The mixed structures are solid solutions of the simple $NiMoO_4$, $CoMoO_4$ and $MnMoO_4$. As far as the mixtures considered are homogeneous in the solid state, the nature of the polymer matrix, the pH of the precursors solution and the relative amount of salt per repeat unit of copolymer seem to have no major effect on the nature of the final phase produced. This result underlines the versatility of the method. Remarkably, the final materials exhibit a very low C content, in spite of using a C-rich organic precursor. Therefore, the approach described here appears as a widely applicable, rather general, method for the preparation of multicomponent oxide-type materials of catalytic or whatsoever interest. It presents an attractive alternative synthetic strategy to materials that could not be prepared easily *via* precipitation, sol–gel or other more classical precursor methods. In addition, compared to other non-conventional methods, the present route offers the advantage of proceeding in aqueous solution.

Acknowledgements

The contribution of D. Chapon (^{13}C-NMR measurements) is greatly acknowledged. FR thanks FNRS (Fonds National de la Recherche Scientifique, Brussels) for a FRIA fellowship. The work was supported in parts by the grant INTAS-00-113, and by a Concerted Research Action of the "Communauté Française de Belgique".

François Rullens,[a] Nicolas Deligne,[a] André Laschewsky*[bc] and Michel Devillers*[a]
[a]*Unité de Chimie des Matériaux Inorganiques et Organiques, Université catholique de Louvain, Place Louis Pasteur, 1l3, B-1348 Louvain-la-Neuve, Belgium. E-mail: devillers@chim.ucl.ac.be; Fax: +32 10 47 23 30; Tel: +32 10 47 28 27*
[b]*Fraunhofer-Institute for Applied Polymer Research, Geiselbergstraße, 69, D-14476 Potsdam-Golm, Germany. E-mail: andre.laschewsky@iap.fhg.de; Fax: +49 331 568 3000; Tel: +49 331 568 1327*
[c]*Universität Potsdam, Institut für Chemie, Karl Liebknecht-Straße, 24-25, D-14476 Potsdam-Golm, Germany. E-mail: laschews@rz.uni-potsdam.de; Fax: +49 331 977 5054; Tel: +49 331 977 5225*

References

1 M. Alifanti, B. Baps, N. Blangenois, J. Naud, P. Grange and B. Delmon, *Chem. Mater.*, 2003, **15**, 395–403.
2 H. Yamamura, A. Watanabe, S. Shirasaki, Y. Moriyoshi and M. Tanada, *Ceram. Int.*, 1985, **11**, 17–22.
3 H. Wullens, D. Leroy and M. Devillers, *Int. J. Inorg. Mater.*, 2001, **3**, 309–321.
4 H.-B. Park, H.-J. Kweon, Y.-S. Hong, S.-J. Kim and K. Kim, *J. Mater. Sci*, 1997, **32**, 57–65.
5 J. C. W. Chien, B. M. Gong, Y. Yang, Y. Cabrera, J. Effing and H. Ringsdorf, *Adv. Mater.*, 1990, **2**, 305–309.
6 K. Naka, Y. Tanaka, K. Yamasaki, A. Ohki, Y. Chujo and S. Maeda, *Bull. Chem. Soc. Jpn.*, 2001, **74**, 571–577.
7 G. Cárdenas and J. Acuna, *Int. J. Polym. Mater.*, 1995, **29**, 147–155.
8 M. Galin, E. Marchal, A. Mathis, B. Meurer, Y. M. Monroy Soto and J. C. Galin, *Polymer*, 1987, **28**, 1937–1944.
9 P. Köberle and A. Laschewsky, *Macromolecules*, 1994, **27**, 2165–2173.
10 P. Favresse and A. Laschewsky, *Polymer*, 2001, **42**, 2755–2766.
11 N. Bonte, A. Laschewsky, B. Mayer and V. Vermylen, *Macromol. Symp.*, 1996, **102**, 273–280.
12 Ph. Favresse and A. Laschewsky, *Macromol. Chem. Phys.*, 1999, **200**, 887–895.
13 F. Rullens, M. Devillers and A. Laschewsky, *J. Mater. Chem.*, 2004, **14**, 3421–3426.
14 F. Rullens, M. Devillers and A. Laschewsky, *Macromol. Chem. Phys.*, 2004, **205**, 1155–1166.
15 S. Kumaresan and P. Kannan, *Indian J. Chem. Technol.*, 2003, **10**, 180–185.
16 P. Ferruti, M. A. Marchisio and R. Barbucci, *Polymer*, 1985, **26**, 1336–1348.
17 L. H. Gan, N. K. Goh, B. Chen, C. K. Chu, G. Roshan Deen and C. H. Chew, *Eur. Polym. J.*, 1997, **33**, 615–620.
18 D. L. Stern and R. K. Grasselli, *J. Catal.*, 1997, **167**, 550–559.
19 L. M. Madeira, M. F. Portela and C. Mazzocchia, *Catal. Rev.*, 2004, **46**, 53–110.
20 A. F. Thünemann, K. Sander, W. Jaeger and R. Dimova, *Langmuir*, 2002, **18**, 5099–5105.
21 M. Hahn, W. Jaeger, R. Schmolke and J. Behnisch, *Acta Polym.*, 1990, **41**, 107–112.
22 M. Hahn, J. Kötz, K.-J. Linow and B. Philipp, *Acta Polym.*, 1989, **40**, 37–43.
23 E. R. Braithwaite and J. Haber, *Molybdenum: An Outline of its Chemistry and Uses*, Elsevier, Amsterdam, 1994.
24 P. Favresse and A. Laschewsky, *Macromol. Chem. Phys.*, 1999, **200**, 887–895.
25 N. Bonte, A. Laschewsky and V. Vermylen, *Macromol. Symp.*, 1997, **117**, 195–206.
26 T. M. Yanushkevich, V. M. Zhukovskii and V. M. Ust'yantsev, *Russ. J. Inorg. Chem.*, 1974, **19**, 1056–1058.
27 T. M. Yanushkevich, V. M. Zhukovskii and V. M. Ust'yantsev, *Russ. J. Inorg. Chem.*, 1976, **21**, 417–420.
28 J. A. Rodriguez, S. Chaturvedi, J. C. Hanson, A. Albornoz and J. L. Brito, *J. Phys. Chem. B*, 1998, **102**, 1347–1355.

29 A. Maione and M. Devillers, *J. Solid State Chem.*, 2004, **177**, 2339–2349.
30 D. Vie, E. Martinez, F. Sapina, J.-V. Folgado, A. Beltran, R. X. Valenzuela and V. Cortés-Corberan, *Chem. Mater.*, 2004, **16**, 1697–1703.
31 A. Kaddouri, E. Tempesti and C. Mazzocchia, *Mater. Res. Bull.*, 2004, **39**, 695–706.
32 E. Payen, P. Dhamelincourt, J. Dhamelincourt, J. Grimblot and J. P. Bonnelle, *Appl. Spectrosc.*, 1982, **36**, 30–37.
33 M. Woydt, A. Skopp, I. Dörfel and K. Witke, *Wear*, 1998, **218**, 84–95.
34 S. Sheik Salem, *Infrared Phys.*, 1987, **27**, 309–315.
35 G. Lautenschläger, H. Weitzel and H. Fuess, *Z. Kristallogr.*, 1994, **209**, 936–940.
36 E. I. Get'mana and V. I. Marchenko, *Russ. J. Inorg. Chem.*, 1986, **31**, 1207–1210.
37 U. S. Ozkan, M. R. Smith and S. A. Driscoll, *J. Catal.*, 1992, **134**, 24–35.